Journal of Thermal Analysis and Calorimetry, Vol. 59 (2000) 763–774

KINETIC STUDY ON PYROLYSIS OF EXTRACTED OIL PALM FIBER
Isothermal and non-isothermal conditions

J. Guo and A. C. Lua

School of Mechanical and Production Engineering, Nanyang Technological University
639798 Singapore

(Received August 30, 1998; in revised form February 6, 1999)

Abstract

Pyrolysis of extracted oil palm fibers under isothermal and non-isothermal conditions was carried out in a thermogravimetric analyzer. Isothermal curves showed that increasing pyrolysis temperature resulted in a faster pyrolysis and a higher conversion of oil palm fibers into gaseous products. Raw material sizes (below 1.0 mm) had insignificant effects on the isothermal pyrolysis, but the fibers with a size fraction of 1.0 to 2.0 mm resulted in a lesser conversion. Two-step reactions were found in the non-isothermal pyrolysis as evidenced by the presence of two peaks in the derivative thermogravimetry curves. Raw material sizes had no obvious effects on the temperature at which the maximum rate of pyrolysis occurred, but affected the rate of sample mass loss. For the low and high temperature regimes, a three-dimensional diffusion mechanism and a first-order of reaction mechanism respectively were used to describe the non-isothermal pyrolysis kinetics of extracted oil palm fibers.

Keywords: extracted oil palm fiber, kinetic parameter, pyrolysis, TG

Introduction

Extracted oil palm fiber (or called palm cake fiber), a cheap and abundant biomass produced during the palm-oil milling process, is usually used as boiler fuel or chemical feedstock for solid (char), liquid (aqueous and tar fractions) and gaseous products [1]. Amongst the thermo-chemical conversion processes (e.g. pyrolysis, gasification and combustion), prolysis is recognized as the most promising one since it can be used either as an independent process for fuels and other valuable chemical products or an initial step to gasification or combustion [2, 3]. The development of proper thermochemical conversion processes for extracted oil palm fibers and the set-up of related equipment require the determination of kinetic parameters (activation energy, frequency factor and reaction order) of the pyrolysis process and a detailed understanding of the pyrolysis mechanism.

A thermogravimetric analyzer (TG) is widely used in pyrolysis kinetic studies by an isothermal or non-isothermal method [4]. Koufopanos *et al.* [5] modeled

1418–2874/2000/ $ 5.00

Akadémiai Kiadó, Budapest
Kluwer Academic Publishers, Dordrecht

the pyrolysis kinetics of particles below 1.0 mm of lignocellulosic materials, such as cotton, beech wood, olive husk, hazel nut shell and corn cob, under isothermal and non-isothermal conditions. These two-stage kinetic models were relatively simple and could predict both the reaction rate and char yield for a wide range of pyrolysis parameters with sufficient accuracy. In another study, characterizations on the pyrolysis of different refuse derived fuels (RDFs) under various heating rates were carried out by Cozzani *et al.* [6]. The RDF non-isothermal TG curves showed two distinct mass loss steps, each being attributable to degradation of cellulosic and plastic materials, respectively. A kinetic model based on the assumption that the RDF degradation rate was the weighted sum of the rates of primary reacting species was developed to predict the RDF mass loss and char yield. Antal and Várhegyi [7] established a simple, first-order, high activation energy (238 kJ mol^{-1}) model to accurately describe the pyrolysis of cellulosic substrates. Secondary vapor-solid interactions were found to be the main source of char formed during cellulose pyrolysis. When a whole biomass substrate was pretreated to remove mineral matter, the pyrolysis kinetics of its cellulose component were very similar to those of pure cellulose.

However, there has been no report about the kinetic studies on the pyrolysis of oil palm solid wastes in the literature. The aim of this paper was to analyze the reaction kinetics on the pyrolysis of extracted oil palm fibers under isothermal and non-isothermal conditions using TG. The effects of raw material size, pyrolysis temperature and heating rate (for non-isothermal study only) on the TG curves and kinetic parameters were investigated.

Experimental

Samples

The extracted oil palm waste was obtained from a palm-oil mill in Selangor, Malaysia. The extracted oil palm fibers consisted mainly of palm long fibers and small impurities of palm peels and palm stone particles. These wastes were air-dried to reduce moisture absorbed during land-dumping. Subsequently, they were cut, ground with a commercial food processor (E262, Philips) and sieved to several size fractions: less than 0.3, 0.3–0.5, 0.5–1.0 and 1.0–2.0 mm. A proximate analysis of the extracted oil palm fiber for a size fraction of 0.5–1.0 mm is given in Table 1.

Table 1 Proximate analysis of the extracted oil palm fiber of 0.5–1.0 mm (wt%)

Sample	Moisture	Volatile matter	Fixed carbon	Ash
Extracted oil palm fiber	6.34	76.20	16.51	0.95

Techniques

The pyrolysis of extracted oil palm fibers was carried out by using a thermogravimetric analyzer (TGA-50, Shimadzu). For isothermal study, approximately 10 mg sample was placed in a platinum pan, which was suspended by a platinum wire. The furnace was heated to a programmed temperature, then the pan was inserted into the furnace. Purified nitrogen (99.9995% pure) at a constant flow rate of 50 cm^3 min^{-1} was used as the purge gas to provide an inert atmosphere for pyrolysis and to remove any gaseous and condensable products evolved, thus minimizing any secondary interactions. The sample was heated by both radiation from the furnace wall and convection of the purge gas flushing through the furnace chamber. For non-isothermal study, the sample was heated at the beginning from ambient temperature to 873 K at a constant heating rate (5 to 30 K min^{-1}). The sample mass was measured continuously by a microbalance as a function of time or temperature.

Determination of kinetic parameters

If the Arrhenius equation is applied to the pyrolysis of biomass, the rate of decomposition reaction can be expressed by the following equation [8]:

$$d\alpha/dt=Kf(\alpha)=A\exp(-E/RT)f(\alpha) \quad (1)$$

where K is the reaction rate constant, A the frequency factor, E the activation energy, R the gas constant, T the absolute temperature, t the time and α the fractional reaction at time t, $f(\alpha)$ is a function that is characteristic of the way the reaction interface proceeds through the sample. The fractional reaction α is defined in terms of the change in mass of the sample,

$$\alpha=(W_0-W)/(W_0-W_f) \quad (2)$$

where W_0, W and W_f are the initial, actual and final mass of the sample, respectively.

Under isothermal condition, the following format is usually use for Eq. (1):

$$d\alpha/dt=K(1-\alpha)^n \text{ or } d\alpha/(1-\alpha)^n=Kdt \quad (3)$$

where n is the reaction order.

Integrating Eq. (3), the following expression can be obtained,

$$[1-(1-\alpha)^{1-n}]/(1-n)=Kt \qquad (\text{for } n\neq 1) \quad (4a)$$

or

$$-\ln(1-\alpha)=Kt \qquad (\text{for } n=1) \quad (4b)$$

For a certain pyrolysis temperature T_i, n_i and K_i can be obtained by linear regression using the data from isothermal curves. Then the activation energy E_0 and frequency factor A_0 can be calculated from a group of T_i and K_i values with least square method.

For the non-isothermal condition with a heating rate q (q=dT/dt), Eq. (1) can be rewritten as follows:

$$d\alpha/dT=f(\alpha)A\exp(-E/RT)/q \text{ or } d\alpha/f(\alpha)=A\exp(-E/RT)/q\,dT \quad (5)$$

Ten alpha functions that are commonly used for biomass decomposition are listed in Table 2. They can be classified into four categories: for 1–3, nucleation and growth are the rate determining process; 4 is based on the reaction order; for 5–6, the geometric nature of the growth of reaction interface is important; for 7–10, diffusion is the rate controlling process [9].

Table 2 Commonly used alpha functions for biomass decomposition reactions

No.	Model	$f(\alpha)$	$g(\alpha)=\int_0^\alpha d\alpha/f(\alpha)$	Label
	Sigmoid rate equations			
1	Avrami-Erofe'ev	$2(1-\alpha)[-\ln(1-\alpha)]^{1/2}$	$[-\ln(1-\alpha)]^{1/2}$	A2
2	Avrami-Erofe'ev	$3(1-\alpha)[-\ln(1-\alpha)]^{2/3}$	$[-\ln(1-\alpha)]^{1/3}$	A3
3	Avrami-Erofe'ev	$4(1-\alpha)[-\ln(1-\alpha)^{3/4}$	$[-\ln(1-\alpha)^{1/4}$	A4
	Based on reaction order			
4	First order	$1-\alpha$	$-\ln(1-\alpha)$	F1
	Based on geometric models			
5	Contracting area	$2(1-\alpha)^{1/2}$	$1-(1-\alpha)^{1/2}$	R2
6	Contracting volume	$3(1-\alpha)^{2/3}$	$1-(1-\alpha)^{1/3}$	R3
	Based on diffusion mechanisms			
7	One-dimensional	$1/(2\alpha)$	α^2	D1
8	Two-dimensional	$[-\ln(1-\alpha)]^{-1}$	$(1-\alpha)-\ln(1-\alpha)+\alpha$	D2
9	Three-dimensional	$3/2(1-\alpha)^{2/3}[1-(1-\alpha)^{1/3}]^{-1}$	$[-\ln(1-\alpha)]^{1/3}]^2$	D3
10	Ginstling-Brounshtein	$3/2[(1-\alpha)^{-1/3}-1]^{-1}$	$1-2\alpha/3-(1-\alpha)^{2/3}$	D4

Integrating Eq. (3), the following expression can be obtained:

$$g(\alpha)=\int_0^\alpha \frac{d\alpha}{f(\alpha)}=\frac{A}{q}\int_0^T e^{(-E/RT)}dT \quad (6)$$

The right-hand side of Eq. (6) has no exact integral, but Eq. (7) can be obtained when this term is expanded into an asymptotic series and higher order terms are ignored.

$$g(\alpha)=ART^2(1-2RT/E)\exp(-E/RT)/qE \quad (7)$$

Taking natural logarithms on both sides of Eq. (7) and assuming that $2RT/E \ll 1$;

$$\ln[g(\alpha)/T^2]=\ln(AR/qE)-E/RT \quad (8)$$

Thus, a plot of $\ln[g(\alpha)/T^2]$ *vs.* $1/T$ will give a straight line of slope $-E/R$ and an intercept of $\ln(AR/qE)$ for an appropriate form of $g(\alpha)$. The criterion used for acceptable values of E and A is that the $f(\alpha)$ should yield the best linear correlation coefficient [10].

Results and discussion

Isothermal study

A series of pyrolysis tests on extracted oil palm fibers at various temperatures from 473 to 873 K with different raw material sizes were carried out in a TG in order to determine the reaction order, rate constant and other isothermal kinetic parameters. Isothermal curves for the pyrolysis of extracted oil palm fibers with a size fraction of 0.5–1.0 mm for various pyrolysis temperatures are shown in Fig. l. At low temperatures of 473 and 573 K, the isothermal pyrolysis lasted quite a long period, but the conversion of extracted oil palm fibers into gaseous products was relatively low (for 473 and 573 K, 17 and 40%, respectively). At these temperature levels, only CO_2 was released as main gaseous product [11]. As the temperature was increased to 673 and 773 K, a faster pyrolysis and a higher conversion ratio could be observed due to a large amount of gaseous products such as CO_2, CO, H_2, and hydrocarbons (i.e. CH_4, C_2H_4, C_2H_6), generated during the pyrolysis process. For the temperature of 873 K, the pyrolysis process was as short as 3 min with the conversion ratio of 85%. At this temperature level, more CO and H_2 and also some high-molecular-mass organic components were released. In brief, the higher isothermal pyrolysis temperature, the faster pyrolysis and the higher conversion of extracted oil palm fibers into gaseous products.

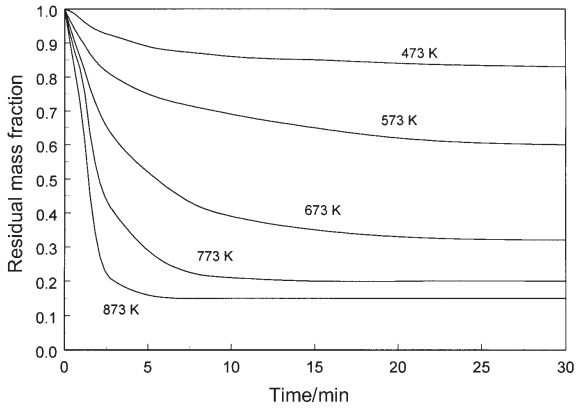

Fig. 1 Isothermal curves for the pyrolysis of extracted oil palm fibers with a size fraction of 0.5–1.0 mm at various temperatures

The effects of raw material size on the isothermal curves for the pyrolysis of extracted oil palm fibers at 673 K are shown in Fig. 2. For the same pyrolysis temperature, the isothermal curves of all size fractions showed a similar trend except for a slight difference among conversion ratios, particularly for the size of 1.0 to 2.0 mm. This was because that for the raw material sizes below 1.0 mm, which belong to fine particles, the pyrolysis of extracted oil palm fibers with these size fractions could be considered to be controlled by pure reaction kinetics, whilst for the fibers between 1.0

to 2.0 mm, the pyrolysis process was controlled by the combination of kinetics and heat transfer, resulting in a lesser conversion [12].

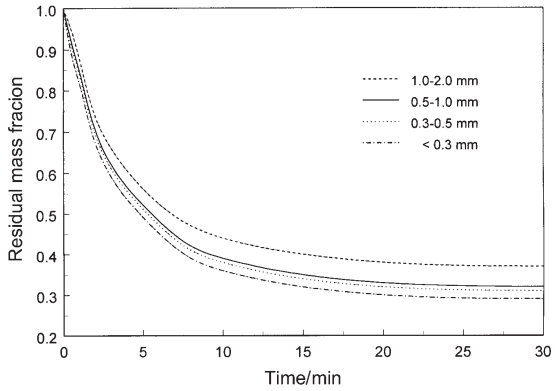

Fig. 2 Isothermal curves for the pyrolysis of extracted oil palm fibers at 673 K with different raw material sizes

Using data from the isothermal curves, rate constant and pyrolysis kinetic parameters (reaction order n, activation energy E_0 and frequency factor A_0) of extracted oil palm fibers of different sizes could be estimated (Table 3). It could be seen from Table 3 that the raw material size had insignificant effects on the pyrolysis kinetic parameters. However, for all sample sizes, increasing isothermal pyrolysis temperature increased the reaction rates significantly, but all values of the reaction order were around 1.0, indicating a first-order reaction of isothermal pyrolysis of extracted oil palm fibers.

Non-isothermal study

Analysis of TG curve

A series of non-isothermal pyrolysis tests on extracted oil palm fibers at a final temperature of 873 K were carried out in a TG with a heating rate varying from 5 to 30 K min^{-1}. A typical TG curve for the non-isothermal pyrolysis of extracted oil palm fibers (raw material size 0.5–1.0 mm) for a heating rate of 10 K min^{-1} and the resultant DTG (derivative thermogravimetry) curve are shown in Fig. 3. The sigmoid curve showed that pyrolysis started at around 400 K. It then showed a significant mass loss in which the main decomposition occurred; this was essentially complete by approximately 610 K. Then, a slower rate of further mass loss occurred until 820 K, after which there was no more mass change. For the DTG curve, it clearly showed that there existed two steps of reactions which took place in distinct temperature regimes with two peak values. The first step occurred within the range T_1 to T_2 (in Fig. 3, 406.6 to 625.2 K) with the maximum rate of mass loss at T_{max1} (566.2 K), whilst the second step occurred within T_2 to T_3 (625.2 to 821.3 K) with the maximum

Table 3 Rate constant and pyrolysis kinetic parameters for isothermal pyrolysis of extracted oil palm fibers with different sizes

Sample size/ mm	Pyrolysis temperature/ K	Reaction order	Rate constant/ s^{-1}	Activation energy/ kJ mol^{-1}	Frequency factor/ s^{-1}	Correlation coefficient
<0.3	473	1.04	0.0015	23.7	0.40	0.9803
	573	1.08	0.0027			
	673	1.06	0.0050			
	773	1.02	0.0089			
	873	1.05	0.0261			
0.3–0.5	473	1.12	0.0013	23.5	0.39	0.9807
	573	1.09	0.0023			
	673	1.03	0.0046			
	773	1.07	0.0084			
	873	1.10	0.0235			
0.5–1.0	473	1.02	0.0013	23.4	0.38	0.9812
	573	1.07	0.0022			
	673	1.06	0.0048			
	773	1.11	0.0087			
	873	1.08	0.0214			
1.0–2.0	473	1.05	0.0010	23.1	0.29	0.9865
	573	1.13	0.0019			
	673	1.09	0.0038			
	773	1.04	0.0071			
	873	1.07	0.0163			

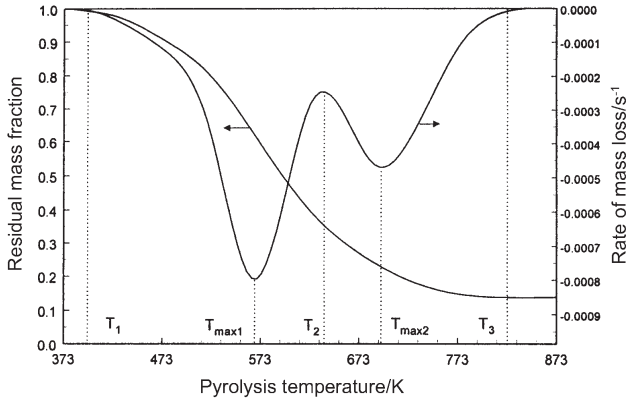

Fig. 3 A typical TG curve for the non-isothermal pyrolysis of extracted oil palm fibers

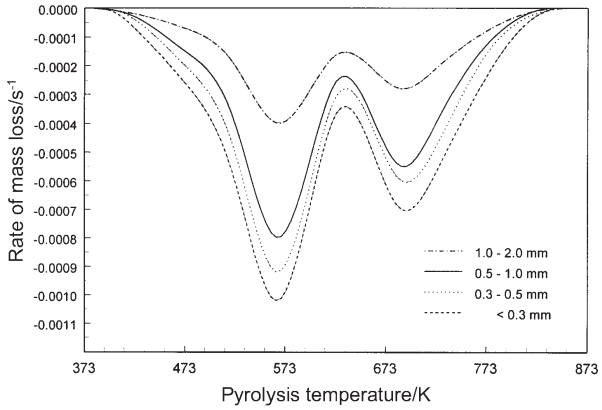

Fig. 4 DTG curves for the non-isothermal pyrolysis of extracted oil palm fibers with different sizes

rate of mass loss at T_{max2} (687.8 K). It had been proposed that the first step was due to the decomposition of hemicellulose, followed by the decomposition of cellulose in the second step [13].

Effect of raw material size

Figure 4 shows the rates of mass change for the non-isothermal pyrolysis of extracted oil palm fibers with different raw material sizes for a heating rate of 10 K min^{-1}. It could be clearly seen that for all sizes, the maximum rates of main mass loss occurred almost at a same temperature $T_{max1}\cong 566$ K), which implied that material size had no obvious effects on the temperature at which the maximum rate of pyrolysis occurred. However, raw material size had an influence on the value of the maximum rate of

mass loss. With increasing size, the rate of mass loss decreased due to reduced release of volatile matters, hence resulting in an increase in the solid residues. Increasing raw material size presented a more tortuous path for the volatile matters to be released and possibly at the same time allowed carbon deposition on the reactive components. Further, heat transfer to the inner surfaces of a larger material size will be less effective as compared to a smaller size, therefore resulting in less energy available to release the volatiles, for otherwise identical operating conditions. Hence, with increase in raw material size, an increase of chars but a decrease of gaseous products would be expected.

Table 4 Pyrolysis kinetic parameters for non-isothermal pyrolysis of extracted oil palm fibers with different sizes

Sample size/ mm	Temperature regime	Activation energy/ kJ mol^{-1}	Frequency factor/ s^{-1}	Correlation coefficient
<0.3		98.2	$3.06 \cdot 10^7$	0.9819
0.3–0.5	low	102.5	$4.79 \cdot 10^7$	0.9851
0.5–1.0		107.6	$6.85 \cdot 10^7$	0.9820
1.0–2.0		142.8	$1.21 \cdot 10^8$	0.9864
<0.3		153.4	$1.09 \cdot 10^{13}$	0.9889
0.3–0.5	high	161.0	$1.43 \cdot 10^{13}$	0.9845
0.5–1.0		166.7	$1.86 \cdot 10^{13}$	0.9872
1.0–2.0		189.3	$2.67 \cdot 10^{14}$	0.9856

Using data from the TG curves, pyrolysis kinetic parameters (activation energy E and frequency factor A) for the non-isothermal pyrolysis of extracted oil palm fibers of different sizes could be calculated (Table 4). In the low temperature regime from T_1 to T_2, pyrolysis model was based on a three-dimensional diffusion mechanism (D3-Table 2) whilst for the high temperature regime from T_2 to T_3, the reaction was based on a first-order of reaction mechanism (F3-Table 2). For both low and high temperature regimes, the size fraction of 1.0–2.0 mm had relatively the highest activation energy, indicating the difficulty of decomposition for this size fraction. For other sample size fractions, the differences of activation energies were relatively small. It appeared that the pyrolysis of raw material sizes less than 1.0 mm, was under pure kinetic control whilst the pyrolysis of larger sizes was probably controlled by the combination of kinetics and heat transfer [14].

Effect of heating rate

Figure 5 showed the mass change *vs*. time curves for the non-isothermal pyrolysis of extracted oil palm fibers (size 0.5–1.0 mm) for different heating rates. It could be seen from Fig. 5 that there was an obvious lateral shift in the TG curves for different heating rates, resulting in delayed decomposition for decreasing heating rate [15]. Temperature ranges of pyrolysis and temperatures at maximum rate of mass loss for different heating rates are listed in Table 5. This table illustrated that the heating rate had

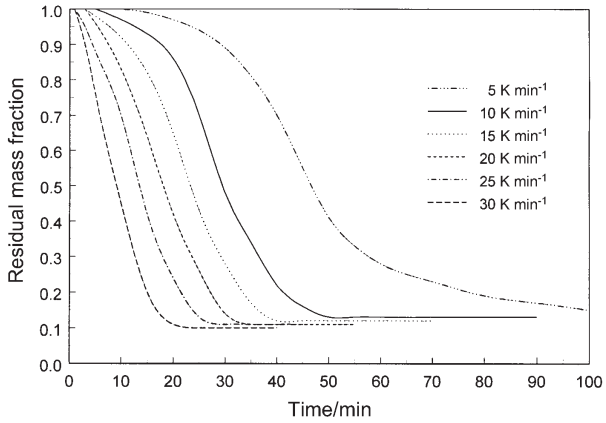

Fig. 5 Residual mass fraction for the non-isothermal pyrolysis of extracted oil palm fibers at different heating rates

influence on not only the temperatures at which the maximum rate of pyrolysis occurred but as well as the starting and ending temperatures for the pyrolysis process. It also confirmed that there was a lateral shift to higher temperatures for T_{max1} and T_{max2} as well as T_1, T_2 and T_3 during the non-isothermal pyrolysis of extracted oil palm fibers as the heating rate was increased. Roman *et al.* [16] investigated the pyrolysis of biomass under heating rates of 40 and 160 K min^{-1} and also found that the total mass loss was mainly affected by the particle size, whilst the temperature at which the maximum rate of pyrolysis occurred was mainly affected by the heating rate.

Table 5 Temperature ranges and temperatures of maximum mass loss for different heating rates

Heating rate/ K min^{-1}	T_1/	T_{max1}/	T_2/	T_{max2}/	T_3/
			K		
5	403.1	555.6	614.8	661.6	820.8
10	406.6	566.2	625.2	687.8	821.3
15	411.5	573.8	634.7	731.8	823.2
20	413.5	578.4	650.4	726.7	831.8
25	414.6	580.6	661.8	737.1	837.5
30	419.9	583.5	672.4	749.7	842.5

Using data from the TG curves for the non-isothermal pyrolysis of extracted oil palm fibers, kinetic parameters at two temperature regimes under different heating rates were calculated (Table 6). As the heating rate was increased, the activation energy and the frequency factor increased from 106.4 to 135.5 kJ mol^{-1} and from $4.00 \cdot 10^7$ to $7.20 \cdot 10^{10}$ s^{-1} respectively for the low temperature regime, whilst for the high temperature regime, the activation energy and the frequency factor decreased from 168.4 to 135.0 kJ mol^{-1} and from $2.11 \cdot 10^{13}$ to $1.03 \cdot 10^{10}$ s^{-1} respectively. In fact, a large number of estimates for the parameters of pyrolysis kinetics of biomass had

been reported in the literature [5]. Reported activation energies varied from 40 to 250 kJ mol^{-1} and fiequency factors from 10^4 to 10^{20} s^{-1}. The large variations in the values reported were mainly due to differences among the various models, the thermal conditions applied and the various materials tested. All the reported kinetic parameters in this paper for the non-isothermal pyrolysis of extracted oil palm fibers under different conditions were within the above ranges.

Table 6 Pyrolysis kinetic parameters for non-isothermal pyrolysis of extracted oil palm fibers at different heating rates

Heating rate/ K min^{-1}	Temperature regime	Activation energy/ kJ mol^{-1}	Frequency factor/ s^{-1}	Correlation coefficient
5		106.4	$4.00 \cdot 10^7$	0.9839
10		107.6	$6.85 \cdot 10^7$	0.9820
15	low	110.7	$1.13 \cdot 10^8$	0.9852
20		117.2	$5.85 \cdot 10^8$	0.9861
25		126.4	$8.66 \cdot 10^9$	0.9877
30		135.5	$7.20 \cdot 10^{10}$	0.9848
5		168.4	$2.11 \cdot 10^{13}$	0.9829
10		166.7	$1.86 \cdot 10^{13}$	0.9872
15	high	158.9	$1.48 \cdot 10^{12}$	0.9856
20		151.3	$9.51 \cdot 10^{11}$	0.9893
25		149.7	$5.80 \cdot 10^{11}$	0.9837
30		135.0	$1.03 \cdot 10^{10}$	0.9884

Effect of pyrolysis temperature

During the non-isothermal stage of pyrolysis (Fig. 5), up to 90% of the volatile matters had been released at the point when the temperature reached the final value of 873 K, indicating that most of the decomposition occurred during the transient heating-up period of the sample. However, pyrolysis temperature did have effects on the activation energy and the frequency factor as could be seen from the two-step reaction during pyrolysis as shown in Tables 4 and 6. In this respect, for the low temperature regime results presented here, pyrolysis was modeled based on a three-dimensional diffusion mechanism (D3-Table 2) as the heating rate was increased from 5 to 30 K min^{-1}. However, for the high temperature regime, the reaction was based on a first-order of reaction mechanism (F3-Table 2).

Conclusions

From the experimental and theoretical studies on the pyrolysis kinetics of extracted oil palm fibers under isothermal and non-isothermal conditions, the following conclusions were drawn:

1. Isothermal curves for the pyrolysis of extracted oil palm fibers from 473 to 873 K showed that increasing the pyrolysis temperature resulted in a faster pyrolysis and a higher conversion of extracted oil palm fibers into gaseous products. For all sample sizes, the reaction order of the isothermal pyrolysis was found around 1.0.

2. A sigmoid mass loss TG curve was found for the non-isothermal pyrolysis of extracted oil palm fibers. However, two steps of reaction existed, characterized by the presence of two peaks for the rates of mass loss in the DTG curves with the first step due to the decomposition of hemicellulose and the second due to the decomposition of cellulose.

3. The raw material size had no obvious effects on the temperature at which the maximum rate of non-isothermal pyrolysis occurred, but affected the value of the rate of mass loss and thus the release of liquid and/or gaseous products and the yield of char.

4. For the low and high temperature regimes, a three-dimensional diffusion mechanism and a first-order of reaction mechanism were found to best describe the non-isothermal pyrolysis kinetics of extracted oil palm fibers respectively.

References

1 B. G. Yeoh, A. Z. Idrus and K. S. Ong, ASEAN J. Sci. Technol. Develop., 5 (1988) 1.
2 A. V. Bridgewater and J. L. Kuester, (Eds), 'Research in Thermochemical Biomass Conversion', Elsevier Applied Science, London 1988.
3 G. Grassi, G. Gosse and G. dos Santos, (Eds), 'Biomass for Energy and Industry', Elsevier Applied Science, London 1990.
4 B. Wunderlich, Thermal Analysis, Academic Press, New York 1990.
5 C. A. Koufopanos, G. Maschio and A. Lucchesi, The Canadian J. Chem. Eng., 67 (1989) 75.
6 V. Cozzani, L. Petarca and L. Tognotti, Fuel, 74 (1995) 903.
7 M. J. Antal Jr. and G. Várhegyi, Ind. and Eng. Chem. Res., 34 (1995) 703.
8 D. Dollimore, W. E. Brown and A. K. Galway, 'Comprehensive Chemical Kinetics', Vol. 22, Bamford, C. H. and Tipper, C. F. (Eds), Elsevier, Amsterdam 1980.
9 M. Reading, D. Dollimore and R. Whitehead, J. Thermal Anal., 37 (1991) 2165.
10 A. Ersoy-Mericboyu, S. Kucukbayrak and B. Durus, J. Thermal Anal., 39 (1993) 707.
11 S. S. Sofer and O. R. Zaborsky, (Eds), 'Biomass Conversion Processes for Energy and Fuels', Plenum Press, New York and London 1981.
12 T. B. Reed, (Eds), 'Biomass Gasification: Principles and Technology', Noyes Data Corporation, New Jersey 1981.
13 P. T. Williams and S. Besler, Fuel, 72 (1993) 151.
14 D. L. Pyle and C. A. Zaror, Chem. Eng. Sci., 39 (1984) 147.
15 A. H. Shamsuddin and P. T. Williams, J. of the Inst. of Energy, 65 (1992) 31.
16 P. Raman, W. P. Walawender, L. T. Fan and J. A. Howell, Ind. Eng. Chem. Process Res. Dev., 20 (1981) 630.